

Hidden photoalignment of liquid crystals in the isotropic phase

E. Ouskova,¹ D. Fedorenko,¹ Yu. Reznikov,^{1,2} S. V. Shiyonovskii,^{2,3} L. Su,² J. L. West,² O. V. Kuksenok,³ O. Francescangeli,⁴ and F. Simoni⁴

¹*Institute of Physics, 46 Prospect Nauki, Kyiv, 03039, Ukraine*

²*Liquid Crystal Institute, Kent State University, Kent, Ohio 44242*

³*Institute for Nuclear Research, 47 Prospect Nauki, Kyiv, 03039, Ukraine*

⁴*Dipartimento di Scienze dei Materiali e della Terra and Istituto Nazionale per la Fisica della Materia, Università di Ancona, Via Breccie Bianche, 60131 Ancona, Italy*

(Received 31 July 2000; published 12 January 2001)

We found the effect of a hidden photoalignment of a dye-doped nematic liquid crystal (LC) on a nonphotosensitive polymer surface after polarized irradiation of the cell in the isotropic phase. We observed that irradiation resulted in a uniform planar orientation of the LC after cooling to the mesophase. The direction of a light-induced easy axis on the polymer can be either parallel or perpendicular to the polarization of the incident light, depending on the light intensity. We attribute this behavior to two mechanisms of photoalignment: light-induced adsorption of dye molecules on the substrate, and anisotropic desorption in a previously adsorbed dye layer. The experimental results on photoalignment of a LC on a thin dye film confirm our model.

DOI: 10.1103/PhysRevE.63.021701

PACS number(s): 61.30.Gd, 68.03.Fg

I. INTRODUCTION

The effects of light-induced alignment and reorientation of liquid crystals (LC's) have been the subject of intense research over the last decade because of the astonishing science and the extremely promising innovative applications [1–4]. One of the most interesting aspects of photoalignment is the possibility of producing an easy-orientation axis on a nonphotosensitive surface in a LC cell upon irradiation by polarized laser light. This effect was first observed in cells filled with dye-doped nematic LC's [5,6]. Recently, a similar effect was observed in a cell filled with a pure pentylcyano-biphenyl (5CB) nematic LC [7,8]. The light intensity needed to align the director of the LC in the dye-doped LC cells was found to be extremely small; energy densities on the order of 0.1 J/cm² were sufficient to write both high-resolution holographic gratings [9,10] and binary images [11]. Therefore, bulk-mediated photoalignment is an extremely promising tool for optical information storage and processing.

The nature of bulk-mediated photoalignment has not yet been finally elucidated, and its microscopic origin is still a subject of open discussion. In Ref. [6] it was proposed that the formation of the easy axis was caused by the anisotropic adsorption of dichroic dye methyl red (MR) molecules onto the illuminated surface during light irradiation (light-induced adsorption). This process is most effective for molecules oriented with their long axes parallel to the light polarization \mathbf{E} . This results in an anisotropic distribution of the adsorbed molecules; hence in the production of the easy axis parallel to \mathbf{E} .

The specific LC effects make light-induced anchoring of a dye-doped LC a difficult subject for study in the mesophase, because the direction in which dye molecules adsorb on a surface depends not only on the light polarization but also on the orientation of the director on the surface [6,12]. In the present work we studied the effect of adsorption-driven photoalignment in the isotropic phase, where there are no director reorientation effects. The irradiation in the isotropic

phase with polarized light results in an anisotropic distribution of the adsorbed molecules. This light-induced anisotropy of the boundary surfaces is hidden in the isotropic state since the adsorbed layer is thin, but it is visualized in the mesophase where LC molecules are oriented along the easy axis produced by adsorbed molecules.

II. EXPERIMENTAL DETAILS AND RESULTS

The experiments were performed using the nematic LC 5CM from Merck doped with the azo-dye MR (Aldrich, weight concentration $\approx 0.5\%$). This photosensitive mixture was used to fill a combined parallel-plane cell consisting of a reference and a test glass substrates. 23- μm spacers were used to control the cell thickness L . The reference substrate was covered with a layer of rubbed polyimide that produced a strong homogeneous planar alignment (i.e., parallel to the rubbing direction) of the LC. The test surface was coated with an isotropic non-rubbed layer of fluorinated polyvinyl-cinnamate (PVCN-F). Before assembling the cell this layer was irradiated with unpolarized UV light from a Hg lamp ($I = 10 \text{ mW/cm}^2$) for about 15 min. This irradiation promoted a cross linking of the polymer chains that makes the polymer surface rigid, and prevented the polymer from dissolving in the LC.

The resulting empty cell was put in a hot stage at $T > T_c$ ($T \approx 50^\circ\text{C}$, $T_c = 34.5^\circ\text{C}$) and was filled with the heated 5CB-MR mixture. The cell was placed normal to the incident Gaussian beam of a He-Cd laser (wavelength $\lambda = 0.44 \mu\text{m}$, power $P < 10 \text{ mW}$) (Fig. 1). The beam was focused onto the LC layer from the side of the test surface. The diameter d of the laser beam, measured at half-maximum intensity in the plane of the cell, was 0.25 mm. The cell was irradiated at different total light intensities, $\bar{I} = 4P/\pi d^2$, for different exposure times t . The polarization of the beam, \mathbf{E} , was set at 45° to the rubbing direction in the cell. After exposure the cell was slowly cooled down to the nematic phase at room temperature. The irradiated areas were exam-

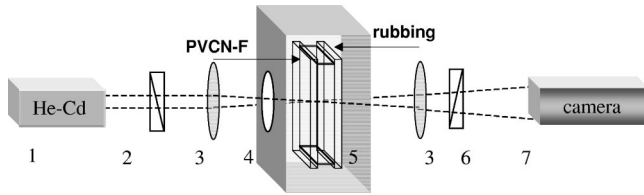


FIG. 1. Experimental setup: (1) He-Cd laser, (2) polarizer; (3) lenses, (4) hot stage with optical window, (5) LC cell, (6) analyzer, and (7) screen or CCD camera connected to the computer.

ined with a polarizing microscope.

The experiments showed the appearance of planar twist structures in the irradiated areas in the nematic phase. Analysis of the textures revealed that the director on the reference surface did not change orientation, and the twist structure was caused by the orientation of the director, \mathbf{d} , on the test surface only. The value and sign of the twist angle φ depended on the light intensity and exposure.

We found that a beam with small intensity ($\bar{I} \leq 1 \text{ W/cm}^2$) caused the director to rotate away from \mathbf{E} , i.e., the twist angle between the initial and light-induced directions of the LC on the test surface, φ , was negative all over the irradiated area. At a given intensity, the absolute value of angle φ increased with t and reached a maximum of about 30° (Fig. 2, curve 1).

The areas irradiated with an intensive beam ($\bar{I} \geq 1 \text{ W/cm}^2$) revealed ring-structures (Fig. 3). At the center part of the areas where the intensity was high, the director rotated toward \mathbf{E} , whereas the director rotated away from \mathbf{E} on the periphery where the light intensity was low. The areas with $\varphi > 0$ and $\varphi < 0$ were separated with a black ring with $\varphi = 0$. At a given intensity, the amplitude of the angle φ increased with exposure time t in both parts of the ring structure. It reached a maximum value of 45° in the central region of the area with $\varphi > 0$, and about -30° on the periphery (Fig. 2, curve 2). The diameter of the areas increased with the increasing beam intensity (Fig. 4).

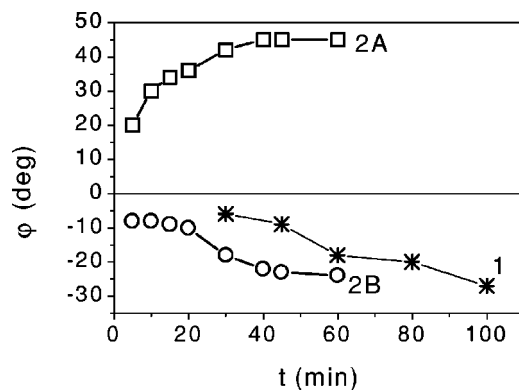


FIG. 2. Twist angle φ vs exposure time t at different intensities. At small intensities ($\bar{I} = 0.12 \text{ W/cm}^2$), the director in the whole spot reorients outwards \mathbf{E} [curve 1 represents $\varphi(t)$ in the spot center]. At high intensities ($\bar{I} = 9 \text{ W/cm}^2$), the director reorients to \mathbf{E} in the spot center (curve 2A), and outward \mathbf{E} in the periphery [curve 2B represents $\varphi(t)$ at the distance 0.25 mm from the spot center].

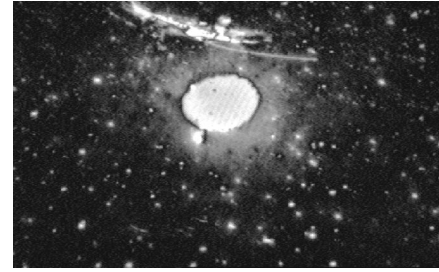


FIG. 3. The ring-twist structure of the area previously irradiated in the isotropic state with intensity $\bar{I} = 8 \text{ W/cm}^2$ and exposure time $t = 1 \text{ h}$. Crossed polarizers, with the polarizer axis parallel to the rubbing direction.

III. DISCUSSION AND ADDITIONAL EXPERIMENTS

The described results show that the irradiation of the cell in the isotropic phase results in a hidden alignment of the LC that can be visualized after transition of the LC to the nematic phase. The orientation of the LC on the tested surface is characterized by the axis of easy orientation of the LC, \mathbf{e} , and the anchoring energy W . The direction of the easy axis corresponds to the minimum of the anisotropic part of surface free energy of the LC. The anchoring energy characterizes the energy required for director deviation from the easy axis. In the case of a distorted LC the director on the tested surface \mathbf{d} does not coincide with the easy axis because of the bulk elasticity of the LC. The larger the anchoring energy the less the deviation of the director from the easy axis, and in the case of a strong anchoring ($WL/K_2 \gg 1$, where K_2 is the twist elastic constant), the directions of \mathbf{d} and \mathbf{e} coincide [13].

At $\bar{I} \leq 1 \text{ W/cm}^2$, \mathbf{d} rotates away from the \mathbf{E} vector with increasing exposure, and the angle φ approaches -30° . This result can be explained if the light-induced easy axis \mathbf{e} is perpendicular to \mathbf{E} , and the light-induced anchoring energy W increases with t . The twist angle φ and anchoring energy W are related as [6]

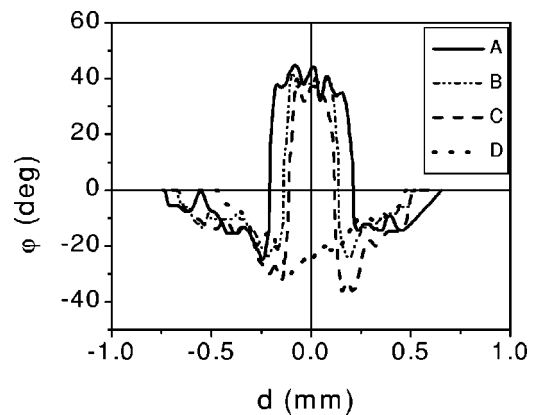


FIG. 4. The spatial distribution of the twist angle φ in the “galo” spot after irradiation in isotropic state at $T = 50^\circ \text{C}$, at different intensities: $\bar{I} = 8 \text{ W/cm}^2$ (A), $\bar{I} = 2 \text{ W/cm}^2$ (B), $\bar{I} = 1.4 \text{ W/cm}^2$ (C), and $\bar{I} = 0.8 \text{ W/cm}^2$ (D). The exposure time $t = 1 \text{ h}$.

$$W = \frac{K_2}{L} \frac{2\varphi}{\sin 2(\theta - \varphi)}, \quad (1)$$

where θ is the angle between \mathbf{e} and the direction of rubbing on the reference surface. For \mathbf{e} perpendicular to \mathbf{E} , $\theta = 45^\circ$, and the maximum value $\varphi = 30^\circ$ corresponds to the value $W \approx 0.3 \mu\text{J}/\text{m}^2$ ($L = 23 \mu\text{m}$, $K_2 = 3.6 \text{ pN}$).

At $\bar{I} \geq 1 \text{ W}/\text{cm}^2$, \mathbf{d} rotates toward \mathbf{E} with increasing exposure, and the angle φ reaches 45° in the center of the irradiated area where the maximum local intensity is. In this case the easy axis \mathbf{e} is parallel to \mathbf{E} . The anchoring energy W increases with the exposure, and strong anchoring is achieved. The value of W depends not only on exposure but also on the intensity. It results in an expansion of the strong anchoring region with increasing \bar{I} .

Thus the direction of the light-induced easy axis on the polymer can be either parallel or perpendicular to the polarization of the incident light, depending on the light intensity. We attribute this behavior to the competition between two mechanisms of photoalignment: light-induced adsorption of dye molecules on the substrate and anisotropic desorption in a previously adsorbed dye layer. The intensity dependence of the director reorientation can be interpreted by the kinetic approach [14]. This approach considers deposition of dye as a relaxation process to a stationary state controlled by adsorption and desorption processes, both affected by light. Motion of dye molecules is considered as Brownian diffusion in the potential field. This field exists near the surfaces due to van der Waals and electrostatic interaction [15]. Specific liquid-crystalline effects caused by the orientational and translational order parameter changes may also contribute to this potential. The characteristic time of adsorption before illumination (dark adsorption) is much longer than the characteristic time of dye diffusion over the cell, and the order parameters increases near the surface. This suggests that the field repulses dye molecules from the surface, and they have to overcome this barrier to reach the surface.

Due to the short-range character of the field, we can separate the thin layer with nonzero potential, and consider the remaining bulk region as a distributed dye source. In this case, the diffusion equation is reduced to the kinetic equations for the surface concentration of adsorbed dye molecules. The properties of the thin layer near the substrate (potential barrier, adsorption, and desorption coefficients) are the controlling parameters in these equations.

The stationary surface concentration of adsorbed molecules \bar{A} on the irradiated substrate and stationary bulk concentration of dye molecules \bar{C} are controlled by the equation

$$\bar{C} = C_0 - \bar{A}/L = \frac{\beta(\bar{A})}{w\alpha(\bar{A})}, \quad (2)$$

where C_0 is the initial bulk density of dye molecules, $w = \exp\{-U/kT\}$ is the Boltzmann factor for surface potential U for dye molecules, and $\alpha(A)$ and $\beta(A)$ are the adsorption and desorption coefficients, respectively. We assume the absence of adsorption on the second substrate. This is also

applicable in the case where the change of bulk concentration due to dark adsorption on the second substrate is negligibly small.

The dependencies of α and β on A are significant, and should be taken into account. When A is small, almost all dye molecules are adsorbed on the bare substrate with the corresponding adsorption coefficient α_0 . When A becomes large, additional dye molecules are adsorbed on the substrate, which has been already covered with the thick adsorbed dye layer, and the adsorption coefficient has another value α_∞ . We approximate $\alpha(A)$ as

$$\alpha(A) = \alpha_\infty + (\alpha_0 - \alpha_\infty) \exp\{-\sigma A\}, \quad (3)$$

where σ is a fitting parameter of the order of area per one molecule. For desorption we use a similar approximation, taking into account that there is no desorption from the bare substrate,

$$\beta(A) = \beta_\infty [1 - \exp\{-hA\}], \quad (4)$$

where h is another fitting parameter of the same order as σ . Light irradiation may affect the dye adsorption and desorption processes through the following mechanisms.

(1) The nonradiative relaxation of the dye excitation right after light absorption results in the local heating of the LC region in the vicinity of the absorbing molecules [16,17]. In addition, reverting to the ground state, dye molecules may change their geometry (trans-cis isomerization). Both effects can decrease the potential barrier near the surface and change the Boltzmann factor as

$$w_{\text{light}} = w_{\text{dark}} \exp(\Delta\nu I), \quad (5)$$

where $\Delta\nu$ is a coefficient of proportionality, and w_{dark} is the Boltzmann factor without light irradiation.

(2) Light absorption by bulk dye molecules, which are close to the substrate, stimulates the adsorption processes. This mechanism affects only the absorbing molecules and its neighbors. Therefore, the light-induced changes of the adsorption and desorption coefficients should be proportional to the intensity I :

$$\alpha_{\text{light}}(A) = \alpha_{\text{dark}}(A)(1 + \Delta\alpha I). \quad (6)$$

(3) Light absorption by dye molecules from the adsorbed layer increases the desorption coefficient the same way:

$$\beta_{\text{light}}(A) = \beta_{\text{dark}}(A)(1 + \Delta\beta I). \quad (7)$$

$\alpha_{\text{dark}}(A)$ and $\beta_{\text{dark}}(A)$ in Eqs. (6) and (7) are the dark adsorption and desorption coefficients, respectively.

The competition between light-induced effects in adsorption (first two mechanisms) and desorption (the third one) results in the different stationary surface concentration of adsorbed molecules \bar{A}_{light} at different irradiation intensity (Fig. 5). If the light-induced adsorption dominates ($\Delta = \Delta\nu + \Delta\alpha - \Delta\beta > 0$), irradiation would increase the thickness of the adsorbed layer (curve 1, $\Delta\bar{A} = \bar{A}_{\text{light}} - \bar{A}_{\text{dark}} > 0$, \bar{A}_{dark} is the stationary concentration of adsorbed molecules without irradiation). If the light-induced desorption is strong enough

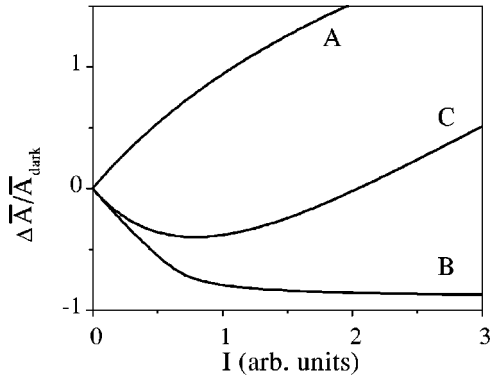


FIG. 5. Dependence of light-induced additional concentration of adsorbed molecules $\Delta\bar{A}$ on light intensity I : (A) $\Delta\nu=0.1$, $\Delta\alpha=0.4$, $\Delta\beta=0.2$; (B) $\Delta\nu=0.1$, $\Delta\alpha=0.1$, $\Delta\beta=0.5$; and (C) $\Delta\nu=0.2$, $\Delta\alpha=0.5$, $\Delta\beta=1$. Dark absorption parameters are $[\beta_{\text{dark}}(\bar{A})/C_0\alpha_{\text{dark}}(\bar{A})]=2\times 10^{-3}$, and $w_{\text{dark}}=\exp(-6)$.

($\Delta < 0$), irradiation would either decrease the thickness of the adsorbed layer for all values of the intensity ($\Delta\bar{A} < 0$, curve 2), or lead to an alternating behavior of $\Delta\bar{A}(I)$: $\Delta\bar{A}$ would be negative for small I and become positive for large I (curve 3).

The presented kinetic model allows us to explain the observed light-induced hidden photoalignment in the isotropic phase. After filling the cell, a layer of adsorbed MR molecules with axially symmetric orientation (dark adsorbed MR layer) grows over the PVCN-F surface. The adsorption and desorption processes determine an equilibrium thickness of this layer. Light action changes this equilibrium thickness and violates the axial symmetry. Because of strong absorption dichroism the dye molecules participating in the light-induced adsorption and desorption processes are predominantly oriented along the light polarization \mathbf{E} . Therefore, light-induced desorption decreases the density of adsorbed molecules parallel to \mathbf{E} , and orients the easy axes perpendicular to \mathbf{E} . At the same time, light-induced adsorption increases the density of adsorbed molecules parallel to \mathbf{E} , and orients the easy axes parallel to \mathbf{E} . Thus a positive light-induced effect in the thickness of the adsorbed layer ($\Delta\bar{A} > 0$) produces a director reorientation toward \mathbf{E} and a negative $\Delta\bar{A}$ leads to a director reorientation outward toward \mathbf{E} .

To show the important role of desorption and to prove the possibility of producing an easy axis in the dark adsorbed MR layer, we carried out the following experiment. A dilute solution of MR (weight concentration $n=0.05\%$, 0.01% and 0.005%) in isopropyl alcohol (IPA) was spin coated on a glass substrate covered with PVCN-F. This PVCN-F was irradiated with unpolarized UV light, and heated at $T=80^\circ\text{C}$ for 30 min. The resulting thin MR-film (thickness between 60 and 200 nm, depending on the MR concentration in the IPA) modeled the layer of MR molecules dark-adsorbed over the PVCN-F surface in the LC cell. Then the MR film was irradiated with polarized light from an Ar^+ laser. The irradiation did not change the shape of the absorption band but just decreased its amplitude (Fig. 6). This find-

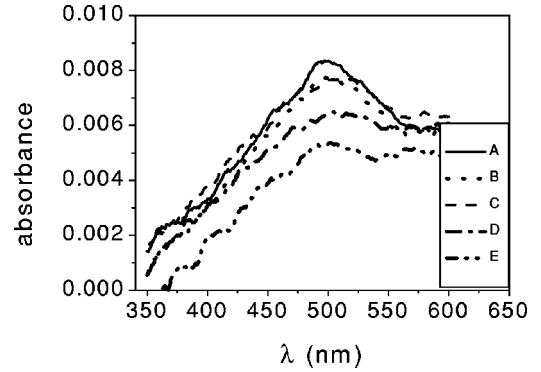


FIG. 6. Dependence of the absorption spectrum of the MR layer on exposure time t : original, $t=0$ (A); $t=10$ min (B); $t=30$ min (C); $t=150$ min (D); and $t=210$ min (E). The concentration of the dye solution is $n=0.005\%$.

ing suggests that light irradiation causes evaporation of MR molecules from the surface.

We assembled the combined cell so that the angle between the rubbing direction on the reference surface and light polarization during exposure was 45° , and then we filled this cell with pure 5 CB in the isotropic state. We observed twist structures in the illuminated areas in the nematic phase. Unlike the previous experiments with the cells filled before irradiation (Fig. 7), the light-induced easy axis was always found to be perpendicular to \mathbf{E} in this case. This result confirms our model because the light-induced adsorption is absent in this experiment, and light-induced evaporation corresponds to the light induced desorption in the filled cell.

IV. CONCLUSIONS

We found the effect of hidden photoalignment of a dyed nematic LC on nonphotosensitive polymer surfaces after polarized irradiation of the cell in the isotropic phase. The results of our experiments can be explained by assuming that after the filling of the cell, a layer of adsorbed MR molecules grows over the PVCN-F surface. Subsequent irradiation of the cell with polarized light results in the development of an anisotropy axis in the adsorbed MR layer because

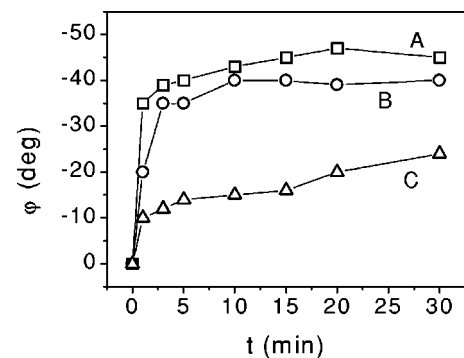


FIG. 7. Twist angle φ vs exposure time t ; the MR film was spin coated from solutions of MR in the IPA with different concentrations n : $n=0.05\%$ (A), 0.01% (B), and 0.005% (C).

of light-induced desorption of dark-adsorbed MR molecules and light-induced adsorption of MR molecules located in the vicinity of the surface. The first process leads to the formation of the easy axis being perpendicular to the polarization of the incident light, while the second process forms the easy axis parallel to the light polarization. Which of the two processes control the final orientation of the easy axis depends on the intensity of the incident light. At low intensities light-induced anisotropy in the adsorbed MR layer prevails whereas at high intensities light-induced adsorption dominates.

This light-induced anisotropy of the boundary surfaces is hidden in an isotropic state, since the adsorbed layer is thin, but it is visualized in the mesophase where LC molecules are oriented along an easy axis given by adsorbed molecules.

We believe that the dye adsorption and desorption processes also control the photoalignment in LC's during irradiation in the nematic phase.

ACKNOWLEDGMENTS

The authors are very thankful to A. Iljin, O. D. Lavrentovich, V. Reshetnyak, and S. Slussarenko for useful discussions. The research described in this publication was made possible in part by NSF ALCOM Grant No. DMR 89-20147, INTAS Grant No. 96-0359, INTAS YSF Grant No. 00-4178 (Ouskova), Grant No. B29/13 of the Fund of the Academy of Sciences of Ukraine, and INCO Copernicus Concerted Action "Photocom" (EC Contract No. ERB IC15 CT98 0806).

-
- [1] W. M. Gibbons, P. J. Shannon, S. T. Sun, and B. J. Swetlin, *Nature (London)* **351**, 49 (1991).
- [2] A. G. Dyadyusha, T. Ya. Marusii, V. Yu. Reshetnyak, Yu. A. Reznikov, and A. I. Khizhnyak, *Pis'ma Zh. Eksp. Teor. Fiz.* **56**, 18 (1992) [*JETP Lett.* **56**, 17 (1992)].
- [3] M. Schadt, K. Schmitt, V. Kozenkov, and V. Chigrinov, *Jpn. J. Appl. Phys.* **31**, 2155 (1992).
- [4] F. Simoni and O. Francescangeli, *J. Phys.: Condens. Matter* **11**, R439 (1999).
- [5] S. T. Sun, W. M. Gibbons, and P. J. Shannon, *Liq. Cryst.* **12**, 869 (1992).
- [6] D. Voloshchenko, A. Khizhnyak, Yu. Reznikov, and V. Reshetnyak, *Jpn. J. Appl. Phys.* **34**, 566 (1995).
- [7] G. Magyar, J. West, Yu. Reznikov, and O. Yaroshchuk, *Mol. Cryst. Liq. Cryst.* **329**, 683 (1999).
- [8] Yu. Reznikov, O. Ostroverkhova, K. Singer, J. H. Kim, S. Kumar, O. Lavrentovich, B. Wang, and J. West, *Phys. Rev. Lett.* **84**, 1930 (2000).
- [9] F. Simoni, O. Francescangeli, Yu. Reznikov, and S. Slussarenko, *Opt. Lett.* **22**, 549 (1997).
- [10] S. Slussarenko, O. Francescangeli, F. Simoni, and Yu. Reznikov, *Appl. Phys. Lett.* **71**, 3613 (1997).
- [11] C. Khoo, M.-Y. Shih, M. V. Wood, B. D. Guenther, P. H. Chen, F. Simoni, S. Slussarenko, O. Francescangeli, and L. Lucchetti, *Proc. IEEE* **87**, 1897 (1999).
- [12] O. Francescangeli, S. Slussarenko, F. Simoni, D. Andrienko, V. Reshetnyak, and Yu. Reznikov, *Phys. Rev. Lett.* **82**, 1855 (1999).
- [13] P. G. de Gennes and J. Prost, *Physics of Liquid Crystals* (Oxford University Press, New York, 1994).
- [14] O. V. Kuksenok and S. V. Shiyonovskii (unpublished).
- [15] F. Garbassi, M. Morra, and E. Occhiello, *Polymer Surfaces* (Wiley, New York, 1997).
- [16] V. N. Sazonov, *Zh. Eksp. Teor. Fiz.* **82**, 1092 (1982) [*Sov. Phys. JETP* **55**, 637 (1982)].
- [17] E. D. Belockii, B. I. Lev, and P. M. Tomchuk, *Mol. Cryst. Liq. Cryst.* **195**, 27 (1991).